Influence of low temperature on the surface deformation of deformable mirrors*

Juncheng You(尤俊成)[1,2,3], Chunlin Guan(官春林)[1,2,†], and Hong Zhou(周虹)[1,2]

[1] *Laboratory on Adaptive Optics, Chinese Academy of Sciences, Chengdu* 610209, *China*
[2] *Institute of Optics and Electronics, Chinese Academy of Sciences, Chengdu* 610209, *China*
[3] *University of Chinese Academy of Sciences, Beijing* 100049, *China*

(Received 11 December 2016; revised manuscript received 7 January 2017; published online 30 March 2017)

The two factors which influence the low temperature performance of deformable mirrors (DMs) are the piezoelectric stroke of the actuators and the thermally induced surface deformation of the DM. A new theory was proposed to explain the thermally induced surface deformation of the DM: because the thermal strain between the actuators and the base leads to an additional moment according to the theory of plates, the base will be bent and the bowing base will result in an obvious surface deformation of the facesheet. The finite element method (FEM) was used to prove the theory. The results showed that the thermally induced surface deformation is mainly caused by the base deformation which is induced by the coefficient of thermal expansion (CTE) mismatching; when the facesheet has similar CTE with the actuators, the surface deformation of the DM would be smoother. Then an optimized DM design was adopted to reduce the surface deformation of the DMs at low temperature. The low temperature tests of two 61-element discrete PZT actuator sample deformable mirrors and the corresponding optimized DMs were conducted to verify the simulated results. The results showed that the optimized DMs perform well.

Keywords: adaptive optics, deformable mirror, thermal effects, testing

PACS: 42.79.Bh, 07.07.Tw, 68.60.Dv **DOI:** 10.1088/1674-1056/26/5/054215

1. Introduction

Turbulence in the earth atmosphere deeply limits the resolution of optical observations.[1] Then adaptive optics (AO) was developed from an original idea by American scientist Babcock to compensate for the atmosphere distortions.[2,3] As shown in Fig. 1(a), in a conventional ground-based telescope, lights from asters are converged on the primary mirror, then reflected by the secondary mirror and a series of reflecting mirrors, finally reach the Coude room where the AO system and the imaging system are working. But the lights from asters passed through the earth atmosphere are very weak. After a series of reflecting, the lights that we can capture may be only counted by photons. Considering this, if the AO system and the imaging system are moved out of the Coude room, the deformable mirror (DM) and tip-tilt mirror (TM) can replace some reflecting mirrors, as shown in Fig. 1(b), then the complexity of the system can be decreased and better images will be obtained. For ground-based telescopes located on the top of mountains, the environment temperature at night when most researches are taken is very low. So the out-of-door AO system will work in a low temperature environment. According to nature temperature data, in the worst situation, the minimum environment temperature is −20 °C.

As the core component of the AO system, whether the deformable mirror can work or not in a low temperature environment is an important question. Some researches have been done. In 2001, Dyson *et al.* measured three 37-channel micro-machined deformable mirrors (MMDMs) at cryogenic temperatures ($T = 78$ K) and found that the magnitude of the surface deflection of the mirror could reach up to 10 waves.[4] In 2003, Xinetics Inc. tested a 349-channel cryogenic discrete electrostrictive actuator DM. The peak-to-valley (PV) of the surface was 5 waves at 35 K.[5,6] In 2014, a lightweight unimorph-type DM was examined by Matthias Goy *et al.*, which had a PV around 30 at 86 K.[7] The above experiments have shown that at cryogenic temperatures, DMs have an obvious surface deformation and actuators have lost partial capability. In 2009, Enya *et al.* manufactured a 32-channel cryogenic deformable mirror based on micro electro mechanical system (MEMS) technology ($T = 95$ K).[8] The actuators of this DM almost did not lose capability at cryogenic temperatures because the operation of the MEMS DM is based on Coulomb forces.

DMs for AO systems have been well developed since the early 1970s.[9–14] Compared to other kinds of DMs, DMs based on discrete PZT actuators are among the most popular ones: capability to deliver high force, high accuracy, fast response time, and low power dissipation.[15] So, in this paper, two sample low temperature DMs based on discrete PZT actuators are manufactured to evaluate the thermally induced surface deformation.

*Project supported by the National Natural Science Foundation of China (Grant No. 11178004).
†Corresponding author. E-mail: youjuncheng722078@126.com
© 2017 Chinese Physical Society and IOP Publishing Ltd

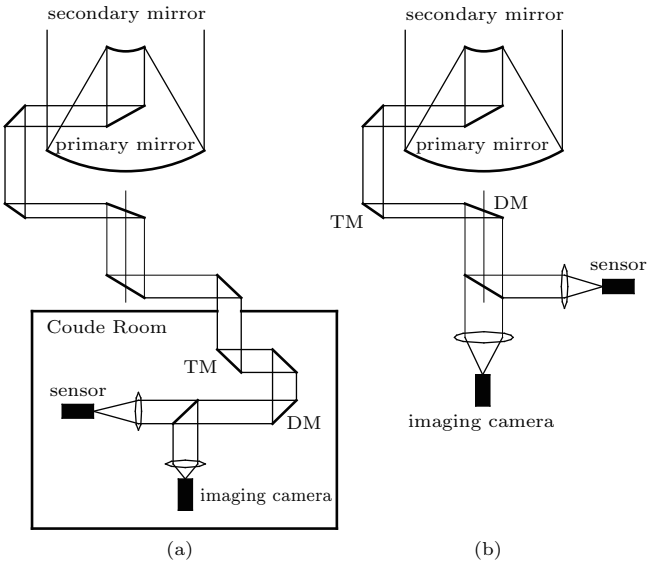


Fig. 1. Schematic diagrams of (a) conventional reflecting telescope and (b) out-of-door reflecting telescope.

From the former researches,[4–8] we know that the two factors which influence the low temperature performance of DMs are the stroke of the actuators and the thermally induced surface deformation of the DM. So the present paper is dedicated to find out the cause of the thermally induced surface deformation of the DMs and find a way to diminish the surface deformation. And we conduct a measurement of surface deformation in low temperature to compare with the theoretical analysis. The piezoelectric stroke of the actuators will be discussed in another paper. The optimized DMs are expected to manifest a surface deformation less than 0.5 waves at -20 °C. In this paper, we just discuss the surface deformation of the DM in an even temperature field.

2. Discrete actuators sample DMs

Two tested sample DMs are room temperature designed 61-element discrete PZT actuators continuous facesheet deformable mirrors. The discrete actuators sample DMs contain three parts: the PZT actuators, the thin facesheet, and the base plate (Fig. 2(a)). They are bonded by epoxy. It is assumed that the bonding is ideal. As shown in Fig. 2(a), PZT is selected to be the actuators; the material of the 2.5-mm thick facesheet is the same as that of the 25-mm thick base plate. The PZT actuators are 10 mm in diameter and 25 mm in height. For the CTE matching, the facesheet of one sample DM is chosen as K4 glass (K4 DM). On the other hand, if the CTE of the facesheet is small enough, the thermally induced surface deformation may be small enough too. So the other facesheet is chosen as ULE (ULE DM). The diameter of the DMs is 150 mm. The clear aperture is 120 mm. The distance between the actuators of these 61-element DMs is 16.4 mm. Figure 2(b) shows the hexagonal arrangement of the PZT actuators. The connection between the DM and the package is flexible.

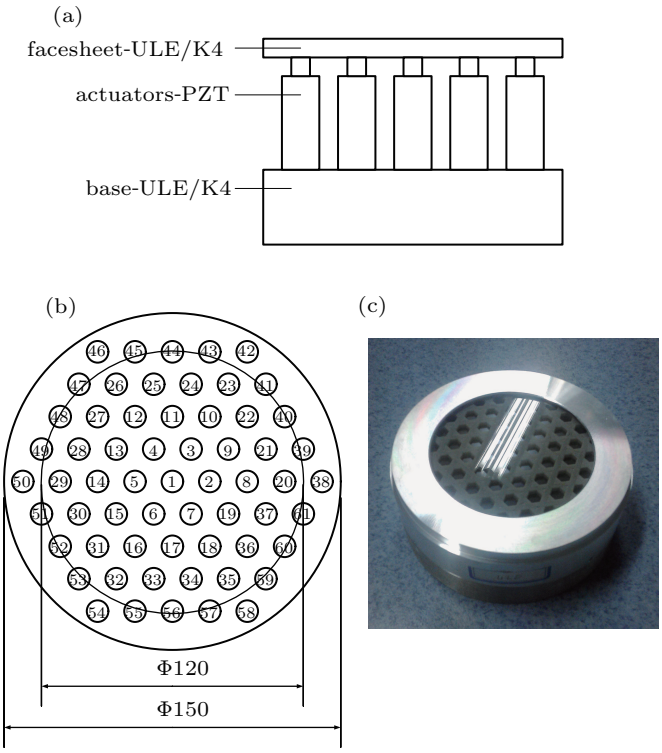


Fig. 2. (color online) Discrete actuators sample DM: (a) the schematic view of DM; (b) the hexagonal arrangement of actuators; (c) abricated DM.

3. Theoretical analysis

3.1. Analysis of the deformation of base

To the best of our previous knowledge, when the thin facesheet and the base plate of DMs adopt the same material, the surface deformation of DMs caused by mismatched CTE between actuators and base should be approximated to zero. In this paper, the CTE mismatching indicates that the CTE of actuators and base is difference. However, an obvious surface deformation of DMs is found during tests in Section 6. So we propose a new theory: in the extreme, when the distance between actuators tends to be zero, then discrete actuators can be seen as a disc. The base plate is stiffer than the thin facesheet, so the discrete actuators DM can be regarded as a bimorph DM. Then at low temperature, the base plate will manifest an unexpected deformation and the facesheet will exhibit an obvious surface deformation. Without regard to the facesheet, because the thermal force caused by mismatched CTE between the actuators and the base is shear force, so the deflection of the base caused by one actuator can be viewed as the response function of the bimorph DM.[16–18] Because the base is a thick plate, so the additional moment caused by the thermal strain cannot be ignored. Figure 3 shows the coordinates of the base.

According to the theory of plates,[19] the additional moment of the base of the DM caused by thermal effects is given by

$$\boldsymbol{M}(T) = \begin{pmatrix} M_x(T) \\ M_y(T) \\ M_{xy}(T) \end{pmatrix} = \int_{-h/2}^{h/2} [\boldsymbol{G}] \begin{pmatrix} \varepsilon_x(T) \\ \varepsilon_y(T) \\ 0 \end{pmatrix} z \mathrm{d}z, \quad (1)$$

where $M_x(T)$ and $M_y(T)$ are the additional bending moments per unit length of sections of a plate perpendicular to the x and y axes, respectively; $M_{xy}(T)$ is the additional twisting moment per unit length of a section of a plate perpendicular to the x axis; $\varepsilon_x(T)$ and $\varepsilon_y(T)$ are the additional thermal strains in the x and y directions caused by mismatched CTE; and T represents the temperature. $[G]$ is given by

$$[G] = E \begin{bmatrix} \frac{1}{1-\nu^2} & \frac{\nu}{1-\nu^2} & 0 \\ \frac{\nu}{1-\nu^2} & \frac{1}{1-\nu^2} & 0 \\ 0 & 0 & \frac{1}{2(1+\nu)} \end{bmatrix}, \quad (2)$$

where E is the elastics modulus, and ν is the Poisson ratio.

The additional moments $M_x(T)$ and $M_y(T)$ will bend the base of the DM. So, the base of the DM will show a shape of hollow or bulge which results into the surface deformation of the facesheet. When the CTE of the base and the facesheet is similar to that of the actuators, the deformation of the base caused by the thermal strain will be less.

In a word, the main cause of the surface deformation of DM is the CTE mismatching induced deformation of the base.

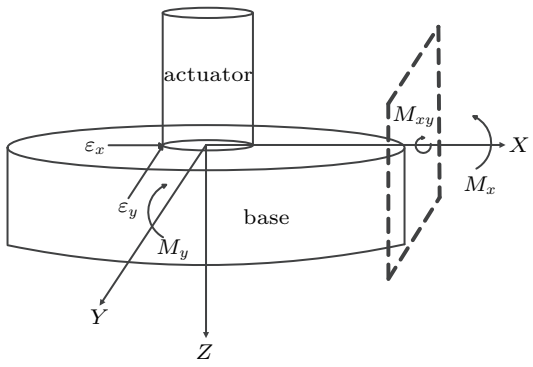


Fig. 3. Coordinates of the base.

3.2. Simulations

The thermally induced surface deformation results from the deformation of the base caused by CTE mismatching. To prove this, the finite element method (FEM) was used to analyze the surface deformation of DMs. The properties of the materials in DMs from −20 °C to 20 °C are listed in Table 1. The CTE of K4, PZT, and ULE from −20 °C to 20 °C was measured through a horizontal push-pod dilatometer. Figure 4 shows the measured length change at different temperatures. The CTE used in simulations was calculated at each temperature point. Figure 5 shows the mesh of the 61-element DM in Ansys workbench. The DM is elastic supported at the base. In this paper, the surface deformation indicates the surface difference of DMs between actual temperature and reference temperature which is 20 °C.

In order to evaluate the CTE mismatching induced upper surface deformation of the base, ULE DM was chosen to be the analysis object, of which the deformation is more obvious than K4 DM. Figure 6 shows the surface deformation of the base produced by actuator 1 and all actuators at −20 °C. We can find out that the CTE mismatching between actuator 1 and the base leads to a sharp deformation of the base in the diameter of the actuator, and a mild deformation of the base out of the diameter of the actuator. So, as shown in Fig. 6, the superposition of 61 unit actuators induced deformation will result in an obvious deformation of the base, which leads to the surface deformation of the facesheet. The upper surface deformation of the base plate contributes to the main part of the thermally induced surface deformation.

Table 1. Material properties of DM from −20 °C to 20 °C.

Material	ρ/kg·m^{-3}	E/GPa	Poisson's ratio	Mean coefficient of thermal expansion/K^{-1}
ULE	2214.4	67.6	0.17	1.50×10^{-8}*
K4	2530	71.4	0.21	4.42×10^{-6}*
PZT	7448	75	0.30	4.62×10^{-6}*

*The CTE of K4, ULE, and PZT at different temperatures were measured.

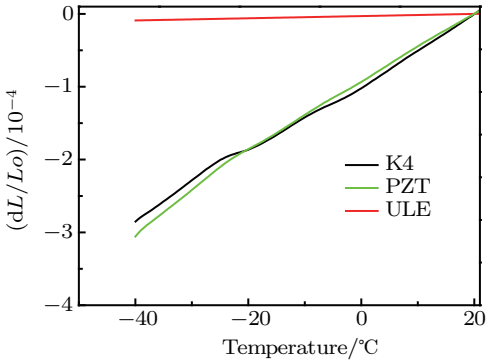


Fig. 4. (color online) Measured length changes of the K4, PZT, and ULE samples.

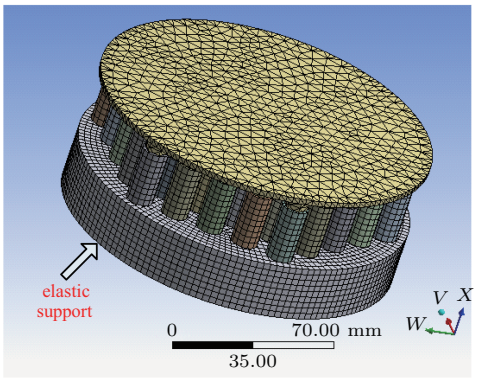


Fig. 5. (color online) Mesh of DM and boundary conditions.

In simulations, the surface of the DMs in 120 mm diameter at 20 °C is flat. So the surface deformation of the DMs is equal to the surface of the DMs at the same temperature. Figures 7 and 8 show the surface deformation of ULE DM and K4

DM from 10 °C to −20 °C in the 120 mm diameter. Comparing the simulated surface deformation of K4 DM with that of ULE DM from 10 °C to −20 °C (Fig. 9), the K4 DM shows an obvious smaller surface deformation than the ULE DM. According to the theory, this is because the CTE mismatching between K4 and PZT is less than that between ULE and PZT. Comparing the surface deformation of the base of the ULE DM at −20 °C in Fig. 6 with that of the facesheet in Fig. 7, we can find that the surface deformation of the facesheet plate is smoother than the upper surface deformation of the base, which is in accordance with the new theory we proposed. The surface deformation of DMs increases as the temperature decreases. The initial PV of the ULE DM surface deformation is 0.142 μm and that of the K4 DM is nearly zero at 10 °C. At −20, the PV of the ULE DM surface deformation is 0.488 μm and that of the K4 DM is 0.129 μm. Because the PV of the ULE DM at −20 °C is greater than 0.5 waves, so an optimization is needed.

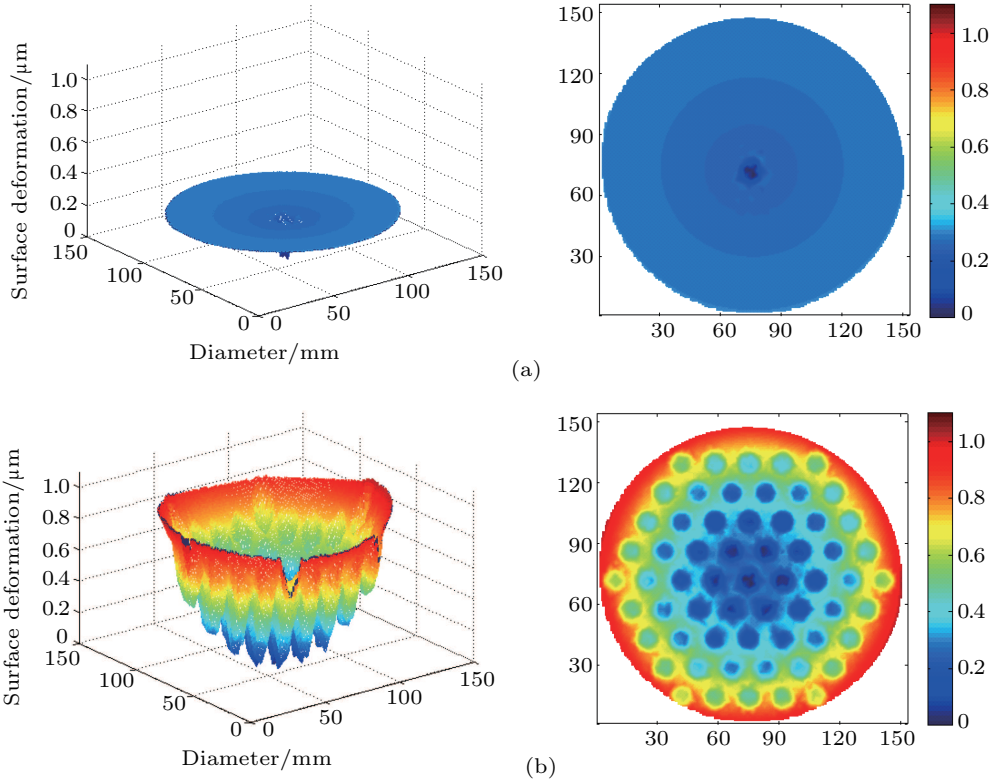


Fig. 6. (color online) Surface deformation of base of ULE DM in 150 mm diameter at −20 °C produced by (a) actuator 1, PV = 0.294 μm; (b) all actuators, PV = 1.041 μm.

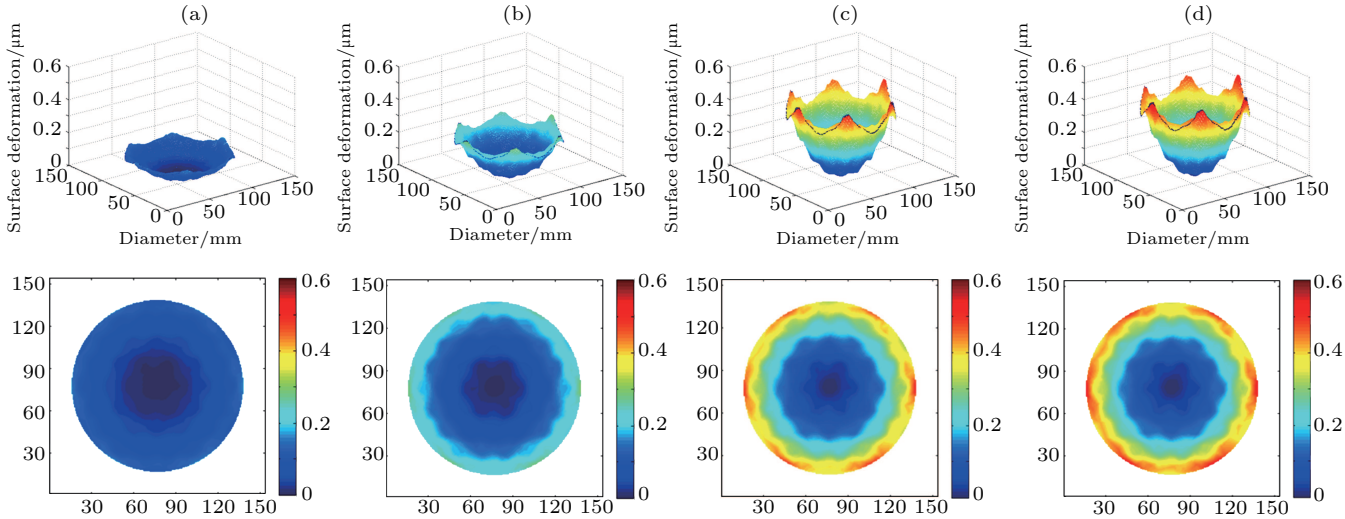


Fig. 7. (color online) Simulated surface deformation of ULE DM in 120 mm diameter: (a) 10 °C PV = 0.142 μm; (b) 0 °C PV = 0.272 μm; (c) −10 °C PV = 0.456 μm; and (d) −20 °C PV = 0.488 μm.

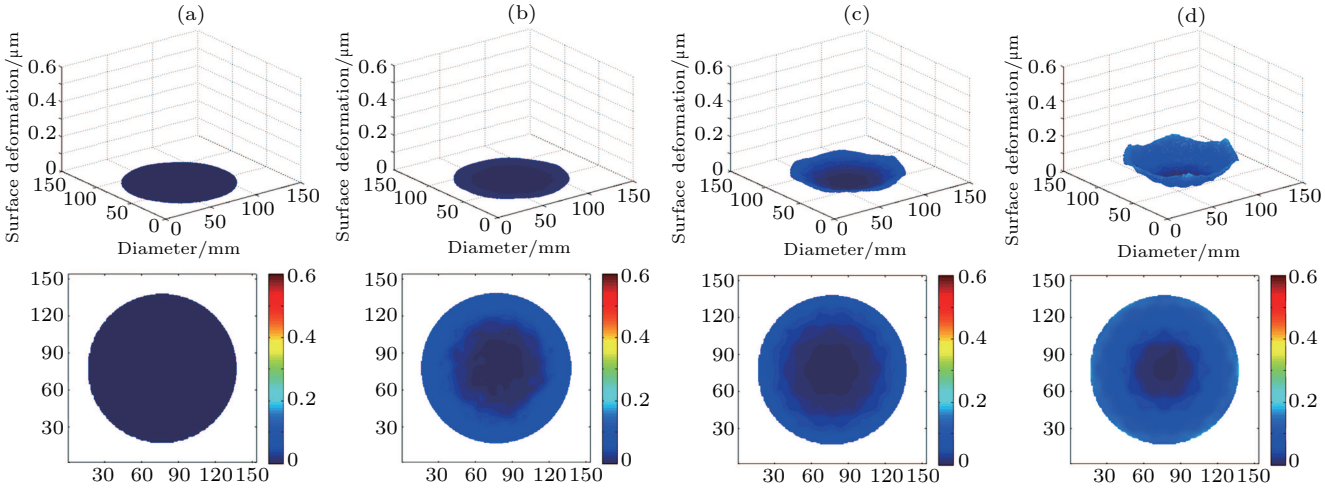


Fig. 8. (color online) Simulated surface deformation of K4 DM in 120 mm diameter: (a) 10 °C PV = 0.008 μm; (b) 0 °C PV = 0.011 μm; (c) −10 ∘C PV = 0.054 μm; and (d) −20 °C PV = 0.129 μm.

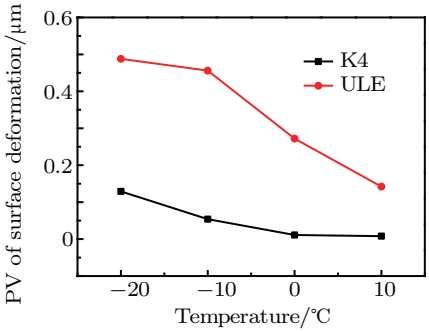


Fig. 9. (color online) PV of simulated surface deformation of K4 DM and ULE DM from 10 °C to −20 °C.

4. Solution

In order to reduce the influence of the mismatched CTE, the base plate of the DM should also adopt an optical head that is the same as the one on the thin facesheet (Fig. 10(a)). The base and the facesheet are both integrated with corresponding optical heads. Based on it, an optimized DM model (Fig. 10(b)) was built in finite element software to analyze the surface deformation of the DMs at low temperature.

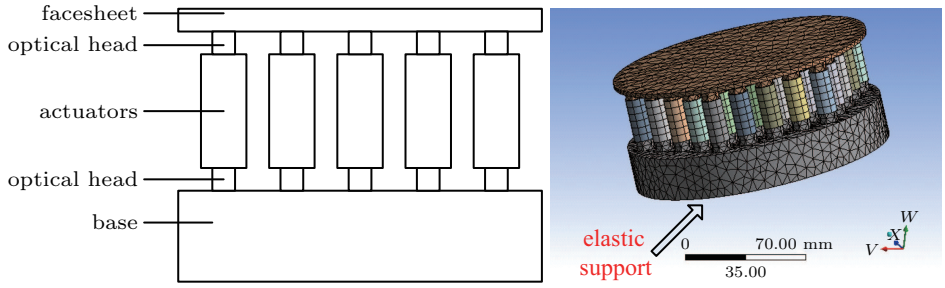


Fig. 10. (color online) (a) Schematic view of the new structure of DM. (b) Mesh of the optimized DM and boundary conditions.

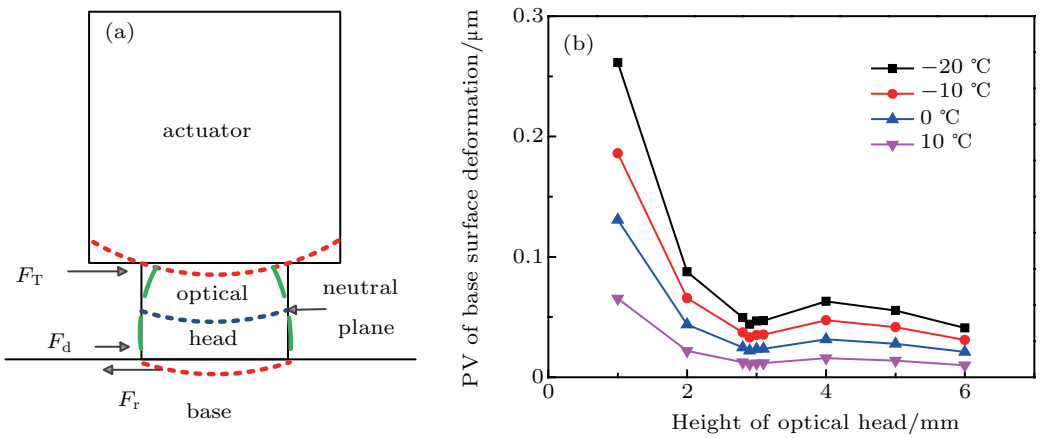


Fig. 11. (color online) (a) Thermal force in the base. (b) PV of base surface deformation of optimized ULE DM with optical head of different heights in 150 mm diameter at different temperatures.

The diameter of the optical head is slightly samller than the diameter of the actuators to satisfy the needs of processing. Therefore, the deformation of the base of the optimized DM is mainly influenced by the height of the optical head. The base surface deformation of the optimized DMs contains two parts: the surface deformation in the diameter of the optical head and the surface deformation out of the diameter of the optical head (Fig. 11(a)). The surface deformation in the diameter of the optical head is mainly caused by the thermal force F_{T} which is radial inward for the optimized ULE DM at the contact plane between the optical head and the actuator. The surface deformation out of the diameter of the optical head is mainly caused by the reacting force F_{r} and decreased thermal force F_{d}. Because the reacting force F_{r} is on the other side of the neutral plane, the reacting force F_{r} which decreases as the height increases is radial outward. According to the Saint Venant's principle, the thermal force F_{T} rapidly decreases along the height direction. When the decreased thermal force F_{d} is equal to the reacting force F_{d}, which decreases slower than the decreased thermal force F_{d}, the surface deformation out of the diameter of the optical head is zero; the surface deformation in the diameter of the optical head also decreases along the height direction. Thus, firstly, the surface deformation of the base will decrease, then increase, and finally decrease. The ULE DM which manifests an obvious surface deformation is chosen to be the simulation objective. The base surface deformation of the optimized ULE DM with an optical head of different heights in 150 mm diameter at different temperatures is simulated, as shown in Fig. 11(b). The simulated results accord with the analysis. The base surface deformation of the optimized ULE DM becomes smoother after 3 mm and the PV reaches the minimum at 6 mm. The height of the optical head on the base is selected as 6 mm. Similarly, the optical head on the facesheet is 6 mm in height. In addition, when the height of the optical head is above 6 mm, the DM will become difficult to manufacture.

Figure 12 shows the simulated upper surface deformation of the base of the optimized ULE DM in 150 mm diameter at −20 °C. Because the DMs have similar shape of surface deformation at different temperatures, so we just plot the simulated surface at −20 °C. The upper surface deformation of the base of the optimized DMs can be seen as flat, comparing with the conventional one (Fig. 6). The deformation direction of the optimized DMs base plate has turned opposite. This is because the direction of the reacting force in the base plate is radial outward. Thus the base plate of the optimized DMs shows an opposite deformation direction, comparing with the conventional one.

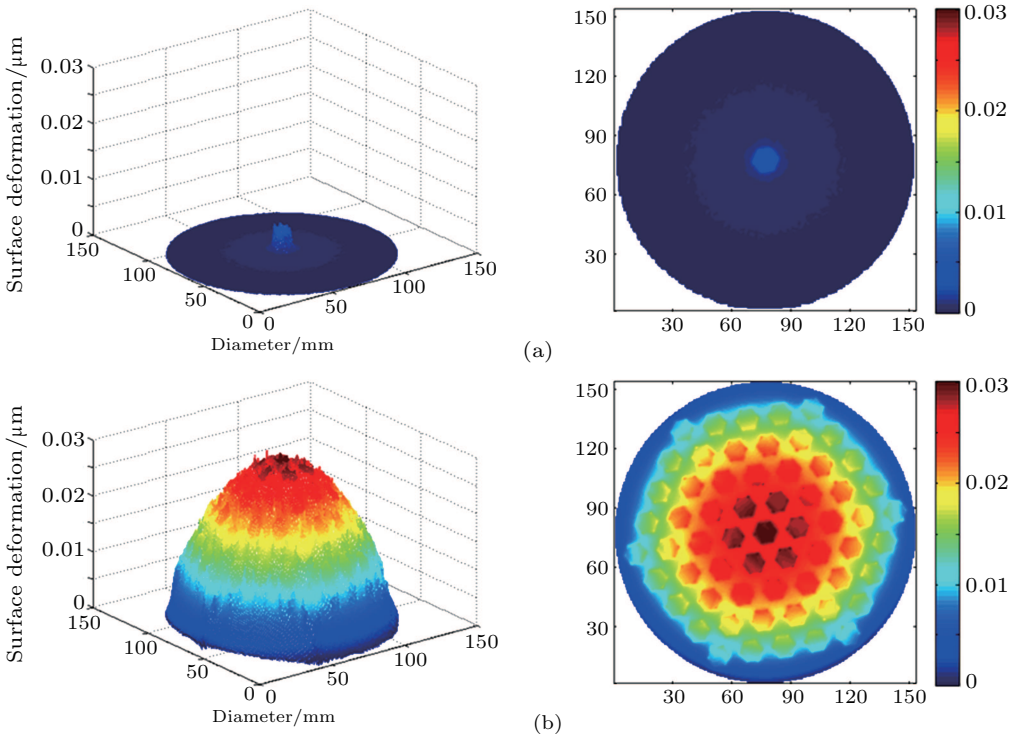


Fig. 12. (color online) Surface deformation of base of optimized ULE DM in 150 mm diameter at −20 produced by (a) actuator 1, PV = 0.005 μm; (b) all actuators, PV = 0.03 μm.

Figure 13 exhibits the surface deformation of the facesheet of the optimized DMs in 120 mm diameter at −20 °C. The surface deformation of the ULE DM outstandingly reduces from 0.488 μm to 0.026 μm at −20 °C after optimizing. The surface deformation of the optimized K4 DM can be ignored. The high order aberrations in the surface deformation of the optimized DMs are caused by the deformation of the optical head. The deformation direction of the optimized DMs has also turned opposite, comparing with the conventional one in Figs. 7 and 8.

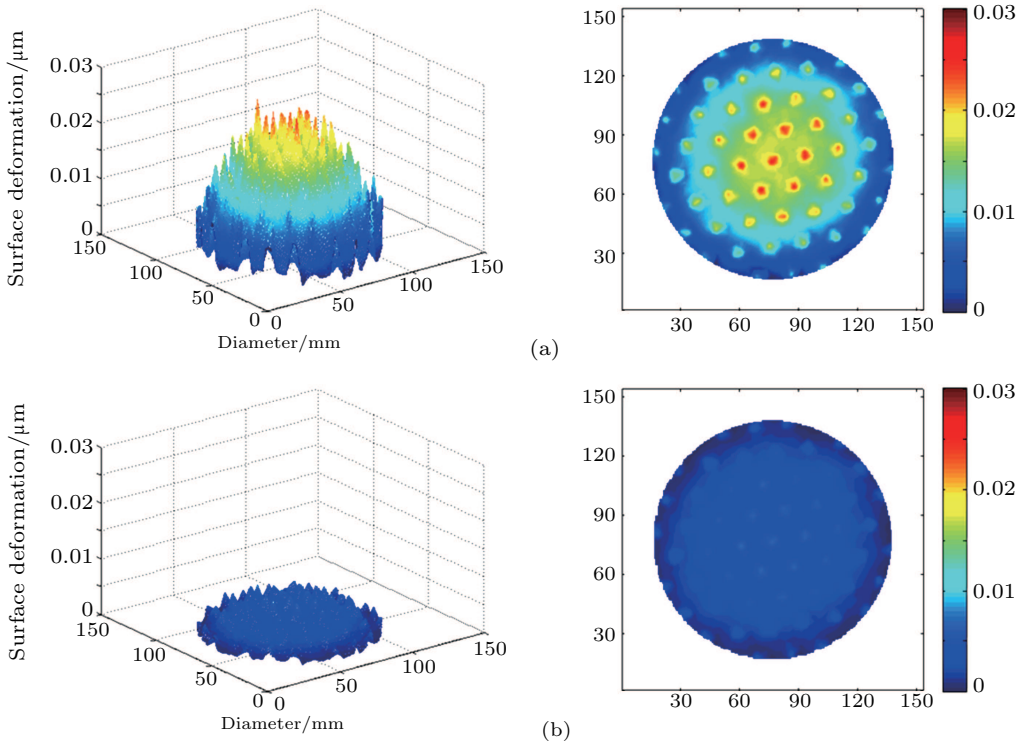


Fig. 13. (color online) Simulated surface deformation of optimized DMs in 120 mm diameter at −20 °C: (a) optimized ULE DM, PV = 0.026 μm; (b) optimized K4 DM, PV = 0.007 μm.

We find out that the optimized DMs manifest a much smoother surface deformation above −20 °C than the conventional DMs and the max PV of the optimized DMs surface deformation is 0.026 μm of the ULE DM at −20 °C. After optimizing, the PV of the ULE DM surface deformation is similar to that of the K4 DM.

The optimized structure of DM can efficiently reduce the surface deformation caused by CTE mismatching. The PV of the optimized DMs at −20 °C is smaller than 0.1 waves.

5. Experiment

Figure 14 shows the low temperature measurement of the DMs. The 4D dynamic interferometer FizCam 2000EP was put out of the cryostat (Fig. 14(a)), where the reference mirror and the DM were mounted in (Fig. 14(b)). According to the working principle of the Fizeau interferometer, the reference light and the objective light both pass through the tailor-made optical window, so the deformation of the optical windows does not influence the measurements. The controllable temperature in cryostat ranges from 20 °C to −20 °C. The wavelength of the light source in the interferometer is 657.2 nm. The collimated light generated by the interferometer reaches the DM/reference mirror, and then is reflected back to the interferometer. The interference fringe was detected by the interferometer, which outputs to the computer. Trapped on a V-shaped groove with buffers, the reference mirror was assumed to be nondeformable when the temperature decreased. The motor driven optical mount where DMs were fixed on can adjust the tilting angle of the DMs through a controller out of the cryostat. The precision of measurement is 0.1 nm.

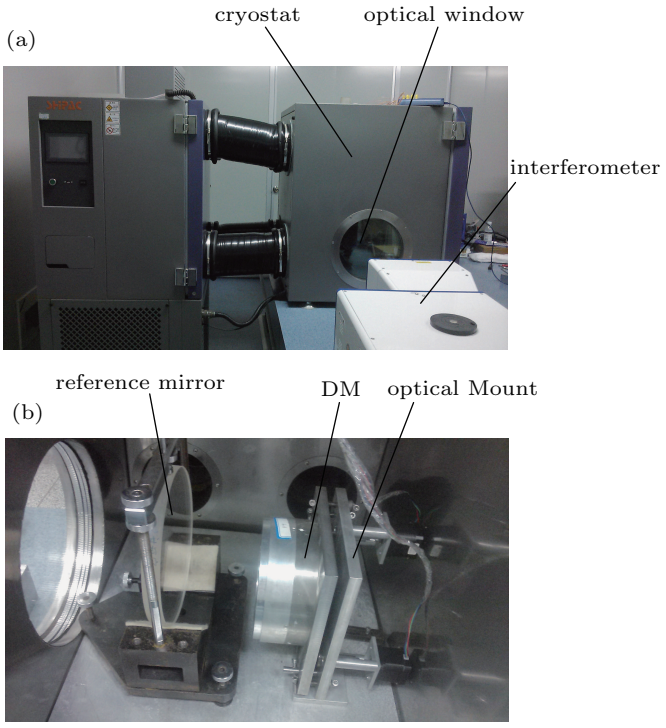


Fig. 14. (color online) DM test setup: (a) interferometer out of the cryostat, (b) standard mirror and DM in the cryostat.

The ambient temperature in the cryostat was held for at least 4 h at 20 °C, 10 °C, 0 °C, −10 °C, and −20 °C to ensure the temperature homogenous of the DMs. Measurement was

taken at five points: 20 °C, 10 °C, 0 °C, −10 °C, and −20 °C. The reference temperature is 20 for tests. The surface deformation indicates the surface difference of the DMs between the test temperature and the reference temperature.

6. Results

The PV of DM surface deformation at different temperatures is given in Table 2. The optimized DMs show a smoother surface deformation than the corresponding conventional DM.

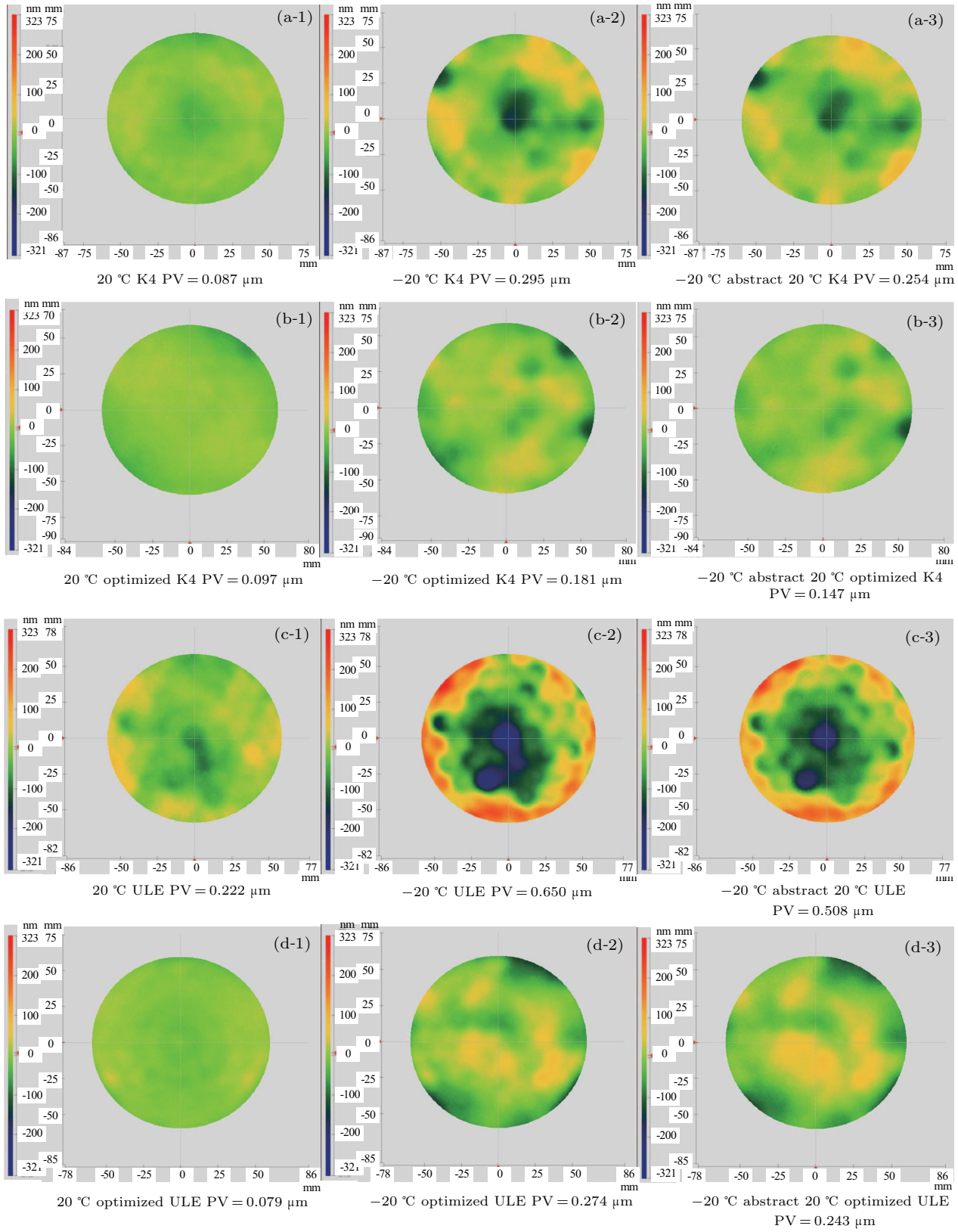


Fig. 15. (color online) Results of tests: (a) K4 DM, (b) optimized K4 DM, (c) ULE DM, and (d) optimized ULE DM. First column is the surface of DMs at 20 °C; second column is the surface of DMs at −20 °C; third column is the surface deformation of DMs at −20 °C.

Table 2. PV of measured surface deformation at different temperatures.

Temperature/°C	PV of surface deformation/μm			
	K4 DM	Optimized K4 DM	ULE DM	Optimized ULE DM
10	0.071	0.043	0.186	0.077
0	0.135	0.079	0.316	0.131
−10	0.180	0.114	0.443	0.196
−20	0.254	0.157	0.508	0.243

At the same temperature, the PV of surface deformation of the ULE DM is almost double of that of the K4 DM; the PV of surface deformation of the optimized ULE DM is nearly the same as that of the K4 DM; the PV of surface deformation of the optimized K4 DM is less than that of the K4 DM. The surface deformation of the DMs indicates a nonlinear variation with temperature. Figure 15 shows the surface of the DMs at 20 °C, −20 °C and the surface deformation of the DMs at −20 °C. Because the DMs show a similar shape of surface deformation at low temperature, so we just plot the surface of the DMs at −20 °C. As it can be seen that the surface of the K4 DM manifests an irregular deformation while the ULE DM manifests a hollow deformation; the surface of the optimized K4 DM is irregular and the optimized ULE DM shows a bulge deformation. Because some PZT actuators destroy the surface of the DMs, so there are obvious high orders aberrations in the surface. Without considering the high orders aberrations, the K4 DM will manifest a hollow deformation and the optimized K4 DM will exhibit a tiny bulge deformation. From the tests, we can find that the optimized DMs efficiently reduce the surface deformation at low temperature.

Comparing the results of simulations with the corresponding tests, we find that the error for ULE DM between simulation and measurement is small enough to be ignored, proving the correctness of the simulation. But the test results of K4 DM, optimized K4 DM, and optimized ULE DM are obviously larger than the simulated results. From Fig. 15, we can find that the error is mainly caused by the inhomogeneous CTE of the PZT actuators. If the difference of CTE is 0.5 ppm/K, then the error caused by the PZT actuators will be 0.125 μm per 10 °C. Because the theoretical surface deformation of these DMs is less than 0.2 μm, so the error caused by the inhomogeneous CTE of PZT may cover the theoretical surface deformation and the actual surface deformation will be obviously larger than the simulated one.

7. Conclusion

In order to find out the cause of thermally induced surface deformation of DMs, a new theory was proposed: without regard to the facesheet, because there are thermal strains between the actuators and the base and the thermal force is shear force, the deflection of the base caused by one actuator can be viewed as the response function of bimorph DM. According to the theory of plates, the additional moments caused by the thermal strain between the actuators and the base will bend the base and the bowing base will result in an obvious surface deformation of the facesheet. So the main cause of the DM surface deformation is the CTE mismatching induced base deformation. The Ansys workbench was used to evaluate the thermally induced surface deformation of DMs. The results proved the correctness of the theory. When the facesheet has a similar CTE with the actuators, the surface deformation of DM would be smoother. An optimized DM design was proposed to reduce the surface deformation of DMs in low temperature. According to the simulation results, the optimized DMs can efficiently reduce the surface deformation and ensure a less than 0.5 waves surface deformation at −20 °C. Two 61-element discrete PZT actuator sample deformable mirrors of 150 mm in diameter and the corresponding optimized DMs were tested from 20 °C to −20 °C. The results showed that the optimized DMs efficiently reduce the surface deformation at low temperature. But error caused by the inhomogeneous CTE of the PZT actuators would cover the theoretical surface deformation of K4 DM, optimized K4 DM, and optimized ULE DM. So the test results of these DMs were obviously larger than the simulated results.

References

[1] Schmutz L E 1993 *Photon. Spectra* **27** 119
[2] Babcock H W 1953 *Publ. Astron. Soc. Pac.* **65** 229
[3] Woolf N 1984 *International Astronomical Union Colloquium* 79*: Very Large Telescopes, their Instrumentation and Programs*, April, 9–12, 1984, Garchingbei Munchen, Germany, p. 221
[4] Dyson H M, Sharples R M and Dipper N A 2001 *Opt. Express* **8** 17
[5] Mulvihill M L, Roche M E, Cavaco J L, Shawgo R J, Chaudhry Z and Ealey M A 2003 *SPIE* **5172** 60
[6] Mulvihill M L, Shawgo R J, Bagwell R B and Ealey M A 2002 *J. Electroceram.* **8** 121
[7] Goy M, Reinlein C, Kinast J and Lange N 2014 *J. Micro-Nanolithogr. MEMS MOEMS* **13**
[8] Enya K, Kataza H and Bierden P 2009 *Publ. Astron. Soc. Pac.* **121** 260
[9] Tyson R K 2010 *Principles of Adaptive Optics* (Abingdon: CRC Press)
[10] Everson J H, Aldrich R E and Albertinetti N P 1981 *Opt. Eng.* **20** 316
[11] Bonora S 2011 *Opt. Commun.* **284** 3467
[12] Uchino K, Tsuchiya Y, Nomura S, Sato T, Ishikawa H and Ikeda O 1981 *Appl. Opt.* **20** 3077
[13] Forbes F, Roddier F, Poczulp G, Pinches C, Sweeny G and Dueck R 1989 *J. Phys. E Sci. Instrum.* **22** 402
[14] Krishnamoorthy R and Bifano T 1995 *Microelectronic Structures and Microelectromechanical Devices for Optical Processing and Multimedia Applications* October 24,1995, Bellingham, USA, p. 96
[15] Madec P Y 2012 *Adaptive Optics Systems III*, July 1–6, 2012, Bellingham, USA
[16] Ning Y, Jiang W H, Ling N and Rao C H 2007 *Opt. Express* **15** 12030
[17] Mehta P K 1990 *Opt. Eng.* **29** 1213
[18] Edric Mark Ellis 1999 *Low-Cost Bimorgh Mirrors in Adaptive Optics* (Ph.D. dissertation) (London: University of London) p. 45
[19] Timoshenko S P and Woinowsky-Krieger S 1959 *Theory of Plates and Shells* (2nd Edn.) (Singapore: McGraw-Hill) pp. 98–100